CERN – European Organization for Nuclear Research
European Laboratory for Particle Physics

ENERGY SPREAD AND ENERGY LOSSES IN CTF3 COMBINER RING

A. Ghigo, M. Zobov

CTFF3 TECHNICAL NOTE

INFN - LNF, Accelerator Division

ENERGY SPREAD AND ENERGY LOSSES IN CTF3 COMBINER RING

A. Ghigo, M. Zobov

1. Introduction

One of the main problems to be solved in the compressor system of CTF3 [1] is to preserve the beam quality. In particular, energy losses and the energy spread are of a great concern for the CTF3 combiner ring design. The energy losses give rise to relative phase errors between bunches through non-perfect ring isochronicity, which result in deterioration of the timing both between individual bunches and merging trains. The energy spread, in turn, leads to bunch lengthening and phase space distortion. Thus, both the energy spread and energy losses can affect strongly the efficiency of the driving beam interaction with transfer structures of the Drive Beam Decelerator.

In Section 2 we discuss the energy spread and losses due to the coherent synchrotron radiation (CSR), while in Section 3 we make an attempt to estimate the combiner ring impedance budget and describe possible design solutions of different vacuum chamber discontinuities aimed at the reduction of the wake fields causing energy loss and energy spread.

Despite the CSR can be also described in terms of the coupling impedance like the "conventional" impedance of the vacuum chamber discontinuities, we intentionally separate these two impedance contributions in the two Sections since they have different impact on the vacuum chamber design. The CSR emission can be decreased by reducing the dimensions of the beam pipe. On the contrary, for the reduction of the conventional wake fields bigger beam pipe sizes are preferable. A reasonable compromise between the contradicting contributions is to be found.

By evaluating the energy spread and the energy losses we keep in mind that according to the design requirements the maximum bunch energy spread acquired in the combiner ring should not exceed ±1% of the nominal energy and the average energy variation along the bunch train must be less than 1%.

2. Coherent Synchrotron Radiation in CTF3 Combiner Ring

Short high charge bunches passing small radius bending magnets of the CTF3 combiner ring can emit coherent synchrotron radiation (CSR) at wavelengths longer than the bunch length. This is the potentially dangerous effect leading to energy spread and loss and, also, to transverse emittance growth.

First analytical evaluations of the effect and numerical simulations in the longitudinal phase space [1] have shown that both energy spread and energy loss due to CSR are tolerable for the ring longitudinal acceptance and allow final bunch compression. These estimates rely on the parallel plate (PP) approximation, i. e. considering a bunch rotating on the circular orbit in the mid plane between two infinite parallel plates, while a real accelerator vacuum chamber is more similar to a thoroidal cavity. So, the validity of the PP approximation should be checked.

On the other hand, the CSR estimates were done for arc cells containing bending magnets with a radius of curvature of 3.6 m and 1.4 m. Instead, we are planning to reutilize the EPA magnets for the combiner ring with the radius of about 1 m. Because of that the estimates are to be repeated.

Contrary to a rather smooth PP impedance [see, for example, 2], the thoroidal chamber (TC) impedance consists of numerous narrow peaks [3]. This means that long lasting TC wake fields can affect multibunch beam dynamics specially taking into account a short bunch separation of 2 cm in CTF3 bunch trains.

There are, at least, two points in favor that the PP approximation is applicable in CTF3 ring case:

1) The TC impedance is shown [3] to be very similar to the impedance of a flat pill-box. Asymptotically, by increasing the pill-box radius its impedance is transformed into the PP impedance [4]. In turn, the PP impedance tends to the free space CSR impedance by increasing the distance between the parallel plates. Thus, one should expect similar wake fields, at least along the bunch length, in the PP case and for the flat thoroidal chamber when the horizontal chamber size is much bigger than the vertical one.

   Indeed, this has been proven by studying CSR in the Compact Storage Ring [5] with the vacuum chamber cross section of 38x80 mm, which is very similar to that proposed for the CTF3 combiner ring, having dimensions of 36x90 mm.

2) A realistic vacuum chamber has a racetrack geometry instead of thoroidal one, i. e. bending sections are interrupted by straight sections. For such a geometry the resonant condition changes leading to resonant peak broadening [6]:

$$\Delta n = \frac{2\pi\rho}{w}\frac{\rho}{l}$$

   where Δn is the peak bandwidth in terms of the revolution harmonic number n (mode number); ρ is the radius of curvature; w is the vacuum chamber width; l is the bending magnet length.

   For CTF3 combiner ring parameters the resonant bandwidth is such that the wake field decays at distance of 1.2 cm behind the bunch and does not affect the next bunches in the bunch train following at a distance of 2 cm.

Figure 1 shows for comparison the real part of the PP impedance and that of the thoroidal chamber with CTF3 ring cross section (which takes into account the resonant peak broadening). Since the wake potential is the convolution integral over the impedance weighted by the bunch spectrum the resulting wake inside the bunch should be very similar for both cases shown in Fig. 1. So, in order to simplify estimates one can safely apply the PP approximation to evaluate the energy spread and the energy loss due to CSR in CTF3 compressor rings.
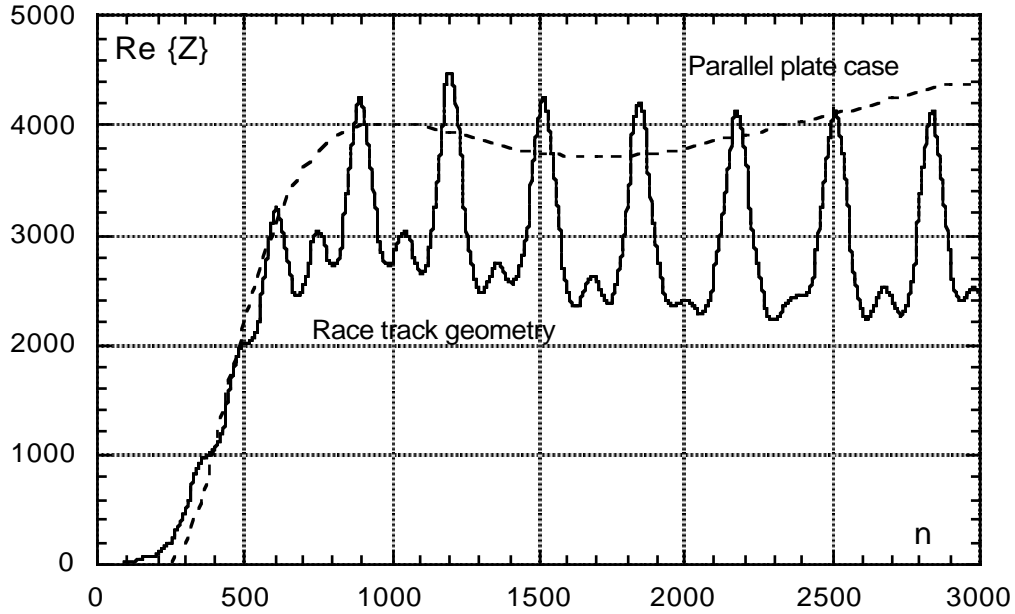
Figure1: Real part of the CSR impedance.

The wake force calculated in eV/m in the PP plate approximation is given by [2]:

$$W(x/\sigma) = \frac{10^{10}}{1.111} \frac{Q}{\left(3\rho^3\sigma^4\right)^{1/3}} \sqrt{\frac{2}{\pi}} \left[\Phi(x) - \left(\frac{3}{4}\right)^{1/3} \Sigma^{4/3} \int\limits_{-\infty}^{+\infty} dy\, G_2(\Sigma y) \exp\left\{ -\frac{1}{2}(x-y)^2 \right\} \right]$$

here Q is the bunch charge ; σ is the bunch length, $G_2(x)$ is the scaling function [see, 2]. The parameter characterizing the PP CSR shielding effect is defined as:

$$\Sigma = \frac{\sigma}{2h}\left(\rho/h\right)^{1/2}$$

2h being the distance between the parallel plates. The function $\Phi(x)$ describing the free space CSR behavior along the bunch is given:

$$\Phi(x) = \Gamma(2/3)\exp\left\{ -\frac{x^4}{4} \right\} D_{1/3}(-x)$$

where $\Gamma(x)$ is the Gamma function and $D_{1/3}(x)$ is the parabolic cylinder function.

Figure 2 shows the wake force calculated for a bunch length of 1 mm, 2 mm and 3 mm, respectively, considering the EPA magnets with ρ = 1.075 m and the distance between the parallel plates 2h = 36 mm.
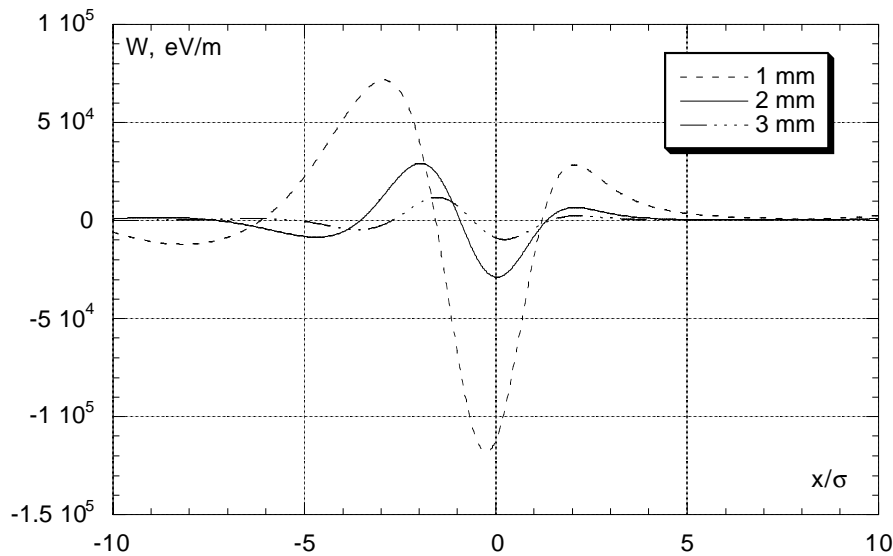
Figure 2: CSR wake force in EPA magnets for different bunch lengths.

Let us estimate the energy spread for a bunch with rms length of 2 mm. As it is seen in Fig. 2 the maximum and the minimum of the wake force have almost the same absolute value of 3x104 eV/m. Taking into account that the CTF3 combiner ring contains 12 bending magnets each 0.5629 m long and in the worst case the bunches make 4.5 turns we can immediately calculate $\Delta E = \pm 0.9$ MeV,or $\Delta E/E \sim \pm 0.5\%$. It means that the energy spread due to CSR is half of that allowable by CFT3 specifications. Comparing in Fig. 2 the wakes of 1 mm and 2 mm bunches we conclude that the energy spread for 1 mm long bunches would exceed the acceptable value. So, bunch stretching before injection into the combiner ring up to 2 mm or preferably higher is necessary to minimize the CSR effect and keep the energy spread within manageable limits.

3. Conventional Impedance Budget and Wake Fields

Besides CSR, an electromagnetic interaction of the beam with a machine vacuum chamber can produce energy spread and energy loss. This interaction is usually described in terms of the frequency dependent impedance or wake fields in the time domain [7]. The vacuum chamber has to be carefully designed in order to minimize the impedance and, thus to avoid excessive energy loss and spread.

Below we list possible impedance contributing elements in the CTF3 combiner ring vacuum chamber:

Phenomena (not discontinuities)

1. Coherent synchrotron radiation
2. Resistive walls
3. Space charge

Big vacuum chamber objects

1. RF deflectors
2. Extraction kickers
3. BPMs or striplines
4. Synchrotron radiation port
5. Injection port
6. Extraction port
7. RF cavity (if decided to be installed)
8. Other

Small vacuum chamber discontinuities

1. Tapers
2. Pumping ports
3. Valves
4. Shielded bellows
5. Flanges
6. Other

Let us evaluate very roughly an acceptable conventional impedance (i. e. excluding the CSR contribution) for the CTF3 combiner ring. Assume that the energy spread should be less than ± 1 MeV after 4.5 turns (ΔE/E~ ±0.5%). Note, that this condition also automatically satisfies the project constraint of having the energy spread along the train below 1%.

For the sake of estimate, we assume an inductive impedance that dominates at low frequencies and induces maximum energy spread along the bunch within ± 1 σ:

$$Z(\omega) = j\omega L; \qquad \frac{Z(\omega)\omega_0}{\omega} = \frac{Z}{n} = j\frac{cL}{R}$$

where ω the angular frequency, ω_0 the angular revolution frequency, n the harmonic number, c the light velocity, L the vacuum chamber inductance and R the average machine radius.

For such an impedance the minimum and maximum of the wake potential inside the bunch are reached at –1 σ and +1 σ, respectively and are given by:

$$W_{max}\left[\frac{V}{C}\right] = -W_{min}\left[\frac{V}{C}\right] = \frac{Lc^2}{\sigma^2 \sqrt{2\pi e}}$$

In order to satisfy the above mentioned requirements on the energy spread for a 2 mm long bunch with a charge of 2.33 nC the vacuum chamber inductance L must be smaller than $1.752 * 10^{-8}$ H and the corresponding normalized impedance Z/n < 0.4 Ω.

However, this estimate can be considered as very approximate. The impedance and the wake potential of vacuum chamber discontinuities can differ much from the inductive one especially for large vacuum chamber objects. Nevertheless, the estimated value compared to the impedance of other accelerator rings (for example, Z/n ~ 21 Ω in EPA [8] and 0.6 Ω in DAΦNE [9]) shows that a very careful design of the CTF3 combiner ring vacuum chamber is necessary to keep the energy spread and losses below the design values.

Since bunches make less than 5 turns in the combiner ring, it is more convenient to consider directly wake fields in the time domain.

<u>Resistive walls</u>

In calculations of the resistive wall contribution we assume that the combiner ring vacuum chamber has a constant cross section with dimensions 2a x 2b = 90 x 36 mm^2. This is the cross section of the vacuum chamber inside bending magnets. Since, in order to avoid many vacuum chamber discontinuities, we are planning to build a smooth vacuum chamber keeping its cross section as constant as possible, this assumption is correct.

The bunch length in the ring is much longer than the characteristic distance s_0 [10]:

$$s_0 = \left(\frac{c\rho b^2}{2\pi} \right)^{1/3}$$

where ρ is the material resistivity. Because of that the long range formulae for the resistive wall impedance and the loss factor k_l per unit length can be safely applied:

$$\frac{\partial Z}{\partial l}(\omega) = (1+j)\frac{\omega}{c}\frac{Z_0\delta}{4\pi b}F_0\left(\frac{b}{a}\right)$$

$$\frac{\partial k_l}{\partial l} = \frac{c}{4\pi^2 b\sigma^{3/2}}\sqrt{\frac{Z_0\rho}{2}}\Gamma\left(\frac{3}{4}\right)F_0\left(\frac{b}{a}\right)$$

where δ is the skin-depth:

$$\delta = \sqrt{\frac{2c\rho}{\omega Z_0}}$$

with Z_0 the free space impedance = 120π Ω. F_0 is a form factor equal to 1 for round beam pipes and differs slightly from 1 for the rectangular cross sections [11].

The wake potential corresponding to the resistive wall impedance and defining the fields distribution inside a bunch is given by:

$$W\left(\frac{s}{\sigma}\right) = Af\left(\frac{s}{\sigma}\right) \qquad \text{where}$$

$$f(x) = |x|^{3/2}\exp\left\{-\frac{x^2}{4}\right\}\left[I_{-3/4}\left(\frac{x^2}{4}\right) - I_{1/4}\left(\frac{x^2}{4}\right) \mp I_{-1/4}\left(\frac{x^2}{4}\right) \pm I_{3/4}\left(\frac{x^2}{4}\right) \right]$$

The numerical coefficient A is defined as:

$$A = \frac{1}{16\pi b}\sqrt{\frac{2\rho Z_0 c^2}{\sigma^3}}$$

and the function -f(x), $I_v(z)$ being the modified Bessel function, is shown in Fig. 3.

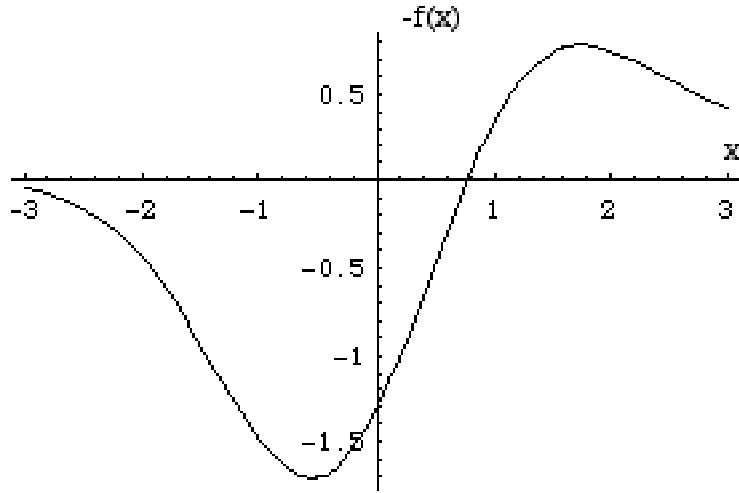Figure 3: Function defining the resistive wall wake potential distribution inside a bunch.

For a numerical estimate we consider b = 18 mm; σ = 2 mm; Q = 2.33 nC; $F_0 \sim 1$; ρ = 2.62*10-8 Ωm (Al). This gives:

$$eQ\frac{k_l}{l} = 29.928\left(\frac{eV}{m}\right)$$

$$eQA = 38.363\left(\frac{eV}{m}\right)$$

It means that after 4.5 turns in the combiner ring, which is 84 m long, the bunch loses 11.312 keV and the energy spread is about 35 keV. These are quite reasonable values. However, if instead of using aluminum one builds a stainless steel vacuum chamber the losses and the energy spread will increase by about a factor of 6 and will no longer be negligible.

Space Charge Impedance

For simplicity let us consider two point charges travelling along a circular beam pipe on trajectories parallel to the pipe axis. If the distances of the leading charge r_1 and the trailing one r from the axis are much smaller than the pipe radius b, the space charge impedance is dominated by its monopolar term [7]:

$$\frac{\partial Z_{m=0}}{\partial l} = -j\frac{\omega Z_0}{2\pi c(\beta\gamma)^2}\left[K_0(\xi r_1) - \frac{I_0(\xi r_1)}{I_0(\xi b)}K_0(\xi b)\right]K_0(\xi r)$$

where $\xi = k/\beta\gamma$; $k = \omega/\beta c$ and I_0 and K_0 are the modified Bessel functions.

By analyzing the behavior of the term in the frequency domain one can note that in the region $\xi b \ll 1$, the impedance per unit length grows linearly, and does not depend on the radial position of the trailing charge:

$$\frac{\partial Z_{m=0}}{\partial l} = -j\frac{\omega Z_0}{2\pi c(\beta\gamma)^2}\ln\left(\frac{r_1}{b}\right)$$

For the combiner ring the conditions ξb <<1 is fulfilled over all the bunch spectrum for bunches with rms sizes of 1 – 3 mm and beam pipe radius of 18 mm.

In the literature the space charge impedance is presented as the space charge monopolar term due to a disk of radius a centered on the pipe axis. Integrating the above expression over the distribution for r_1 between 0 and a for ξb <<1 we get:

$$\frac{\partial Z}{\partial l} = -j\frac{\omega Z_0}{4\pi c(\beta\gamma)^2}\left[1 + 2\ln\left(\frac{b}{a}\right)\right]$$

By substituting the disk radius a by the vertical rms bunch size and taking into account that the geometric aperture is by about a factor of 10 bigger than the transverse rms beam size, i. e. putting the ratio b/a ~ 10, we obtain a rough estimate of the space charge impedance:

$$\frac{Z}{n} \cong -j0.008\Omega$$

This value is much smaller than the imposed impedance limit of 0.4 Ω. Moreover, it has the sign opposite to that of purely inductive impedance due to small vacuum chamber discontinuities. Therefore, in the following we can neglect the space charge contribution to the energy loss and spread.

RF deflectors

The transverse RF deflectors are travelling wave iris loaded waveguides whose fundamental mode is a deflecting hybrid mode with $2\pi/3$ phase advance per cell and negative group velocity. The RF deflector design and detailed analysis of the transverse beam dynamics are given in [12].

Since the deflector structure is azimuthally symmetric except only for the output and input couplers, the 2D ABCI code [13] can be used to calculated the energy spread and loss. Figure 4 shows the ABCI input structure consisting of 10 cells.
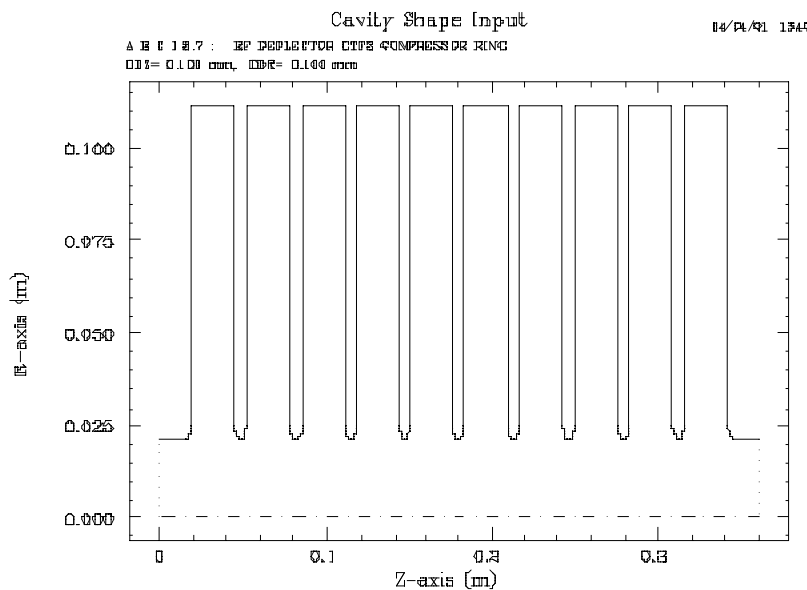

Figure 4: ABCI RF deflector input structure.

The resulting wake potential calculated for a 2 mm long bunch is shown in Fig. 5, while Table I summarizes the loss factors and gives maximum values of the wake potential for different bunch lengths.
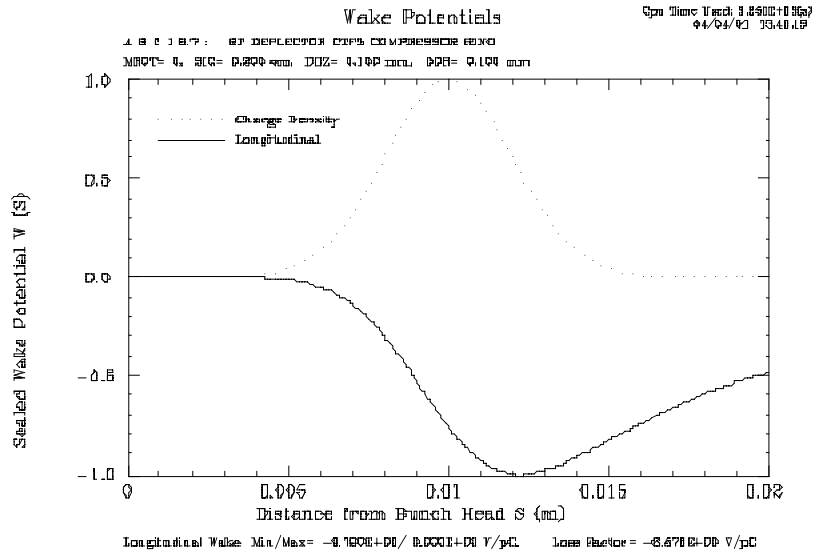

Figure 5: Wake potential of a 2 mm bunch in the RF deflector.

Table I: Loss factors and maximum values of the wake potential

σ, mm	kl, V/pC	|W max|, V/pC
0.5	11.66	15.67
1.0	8.532	11.70
2.0	6.585	9.759
3.0	5.665	8.449

The combiner rings contains two RF deflectors. Thus, we can calculate that a 2 mm bunch with 2.33 nC charge after 5 turns (maximum) loses 153 keV and gains an energy spread from 0 to –227 keV. From the data of Table 1, one can easily scale these data to other bunch lengths.

Extraction kicker

The design and technical parameters of the extraction kicker are discussed in [14]. Here, for sake of estimate we simulate a 2D model of the kicker with the ABCI code. As shown in Fig. 6, for this purpose we substituted the two strip lines by one full coverage strip. This is expected to give a slight overestimate of the final result.

The wake potential for a bunch with 2 mm rms size is shown in Fig.7 and the loss factors and maxima and minima of the wake potential for different bunch lengths are listed in Table II. Now it is easy to calculate that the 2 mm bunch loses 18 keV and accumulates an energy spread of 34 keV due to the extraction kicker after 5 turns in the combiner ring (if we consider a bunch charge of 2.33 nC). Note that the kicker contribution to the losses is much smaller than that of the RF deflectors.
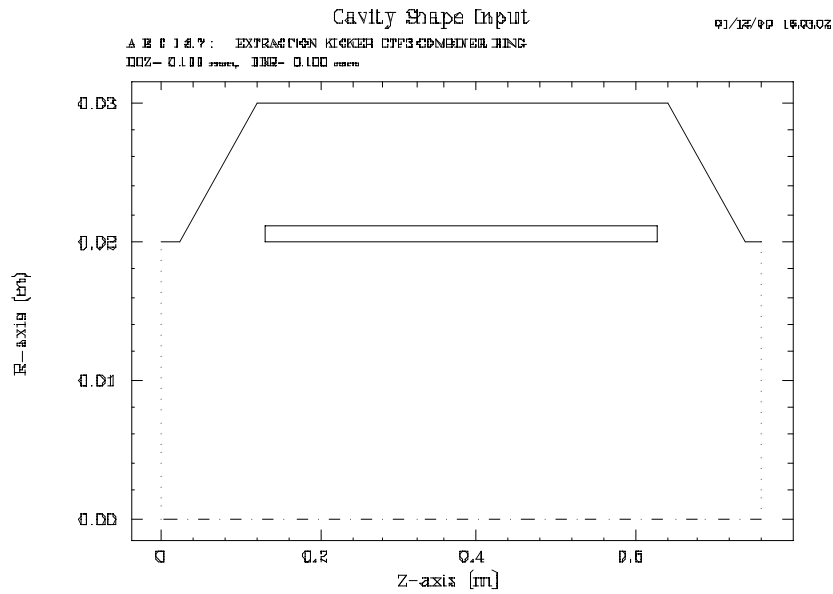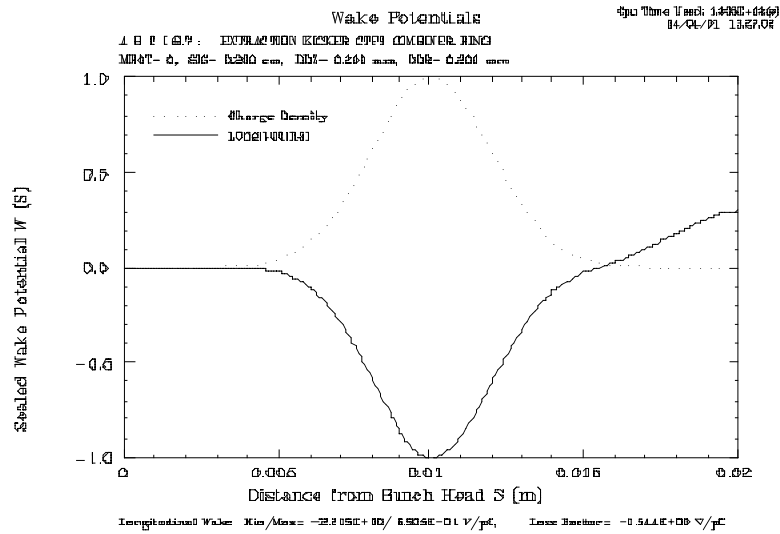
Figure 6: ABCI extraction kicker 2D model.

Figure 7: Extraction kicker wake potential of 2 mm bunch.

Table II: Loss factors, maximum and minimum values of the wake potential

σ, mm	kl, V/pC	W max, V/pC	W min, V/pC
0.5	5.914	0.567	-9.667
1.0	3.008	0.094	-4.205
2.0	1.544	0.69	-2.215
3.0	0.989	0.79	-1.429

BPM

We are planning to employ magnetic pick ups similar to those used for the LEP pre-injector [15] as beam position monitors in the CTF3 compressor rings. Technical performance of such BPMs is described in detail in [16].

The magnetic position monitor consists of a pick up pill-box and the vacuum chamber welded together. A ceramic ring with a resistive metallization inside is used to prevent charge accumulation. Evaluation of the coupling impedance of such a structure is not a simple task. That is why a number of recent papers have been dedicated to both analytical studies [17] and to impedance measurements [18] of BPMs of that kind.

According to bench measurements [19] the maximum value of the normalized impedance Z/n reaches 70 mΩ in a range up to 3 GHz. This high value is a matter of concern since the impedance contribution of 36 BPMs which are to be installed in the combiner ring can exceed the acceptable impedance budget.

However, to get a final answer we have to take into account the following considerations:

- Despite the maximum impedance value is high, one has to consider the actual frequency behavior of the impedance in order to calculate correctly the energy loss and the energy spread.
- The BPM impedance is measured up to 3 GHz, while the frequency spectrum of 1-3 mm bunches goes beyond some tens of GHz. Generally, the impedance above the beam tube cut off decreases with frequency. Moreover, the ceramic metallization is expected to screen completely the BPM for higher frequencies. This means that the effective impedance weighted by the bunch spectrum will be much smaller than the maximum value measured at relatively low frequency.

For sake of estimates we will rely here on the results of the impedance measurements described in [19]. We also assume the impedance beyond 3 GHz vanishes. This assumption can be justified by the fact that we will increase the thickness of the metallization in order to enhance the screening effect at high frequency.

The measured BPM impedance is well approximated by a sum of two broad-band resonances with shunt impedances $R_1 = 26\ \Omega$ and $R_2 = 21\ \Omega$ at the resonant frequencies $f_1 = 1.3$ GHz and $f_2 = 2.3$ GHz, respectively. The resonant modes have low quality factors of $Q_1 = 2.5$ and $Q_2 = 5$.

The real part of the model impedance (shown in Fig. 8) is notably similar to the measured one. The imaginary part is slightly lower, but behaves in the same way as the measured quantity. Now, it is easy to calculate the wake fields corresponding to this resonant impedance applying the standard definitions.

Figure 9 shows the energy loss distribution inside a 2 mm long Gaussian bunch with a charge of 2.33 nC in the range of $-5\ \sigma$; $+10\ \sigma$. As we can see, the maximum energy loss is about 2 keV. So, after 4.5 turns inside the combiner ring containing 36 BPMs the bunch will gain energy spread of about 330 keV. This energy spread is comparable or even higher than the spread due to the RF deflectors, but still does not exceed the design value. We also hope to significantly reduce this amount by increasing metallization thickness.

We should note here another important feature of the BPM wake. Despite the BPM resonant impedance is rather broad, the resulting wake lasts much longer than the distance between bunches in the beam (see Fig. 10). This has to be taken into account when analyzing multibunch dynamics.
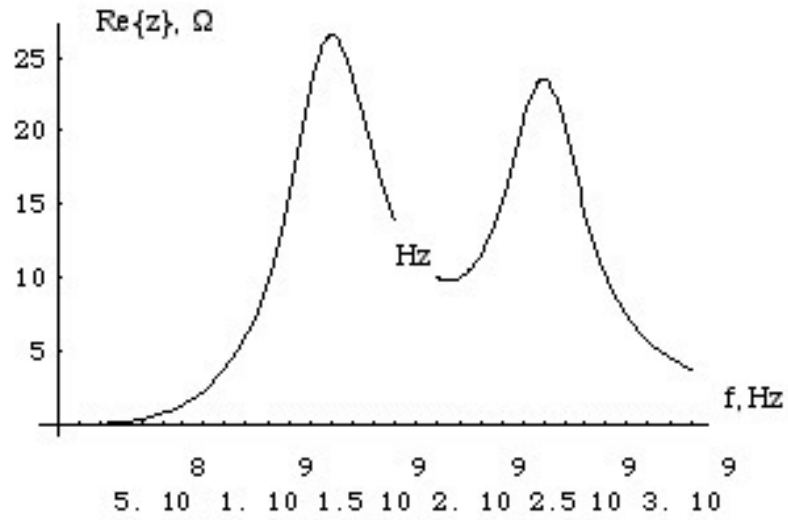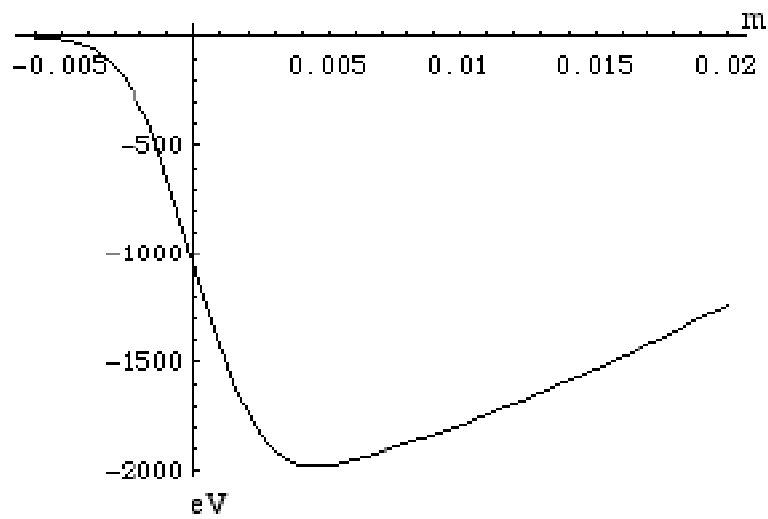
Figure 8: Real part of the BPM impedance.

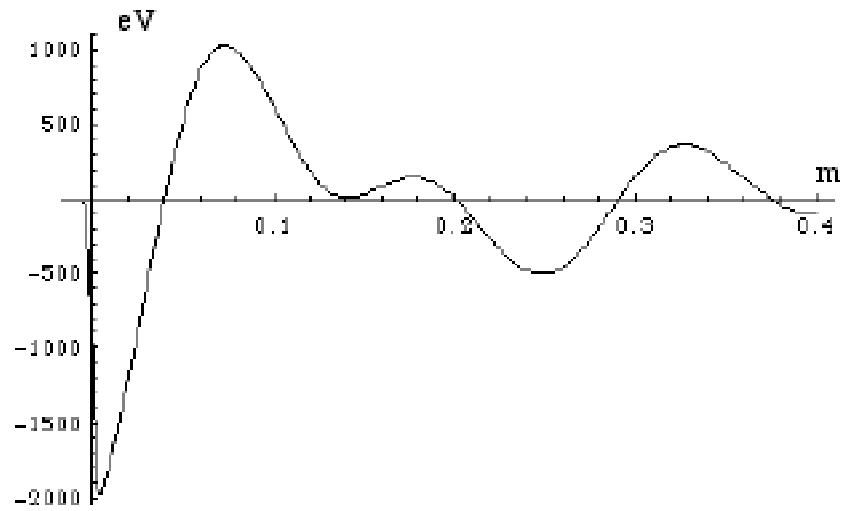Figure 9: Distribution of the energy loss inside 2 mm Gaussion bunch with 2.33 nC charge.

Figure 10: Long range BPM wake fields.

Vacuum port RF screen

In the design of a vacuum port RF screen we use the idea of hidden slots [20] which has been successfully applied for PEP II [21]. This allows to reduce substantially (up to some orders of magnitude) the coupling impedance and prevent radiation into the pump chamber.

Figure 11 shows a sketch of the RF screen. It consists of 38 grooves 72 mm long, 2 mm wide and about 2 mm deep in the rectangular vacuum chamber pipe with 4 mm thickness. Along each groove 25 circular holes with a radius of 1 mm are drilled for pumping purpose. The following features are taken into account in the present design:

- the impedance of long slots saturates when the slots length exceeds 2-3 slot widths. Thus, it is more convenient to use long slots instead of many holes providing the same pumping speed;
- on the other side, for the long slots TE mode travelling wave excited in a ring can radiate into the pump chamber and may damage the pumps and also create resonant HOMs beyond the RF screen.

Therefore, the long grooves are used to decrease the impedance, while the holes prevent penetration of the RF fields outside the beam pipe.
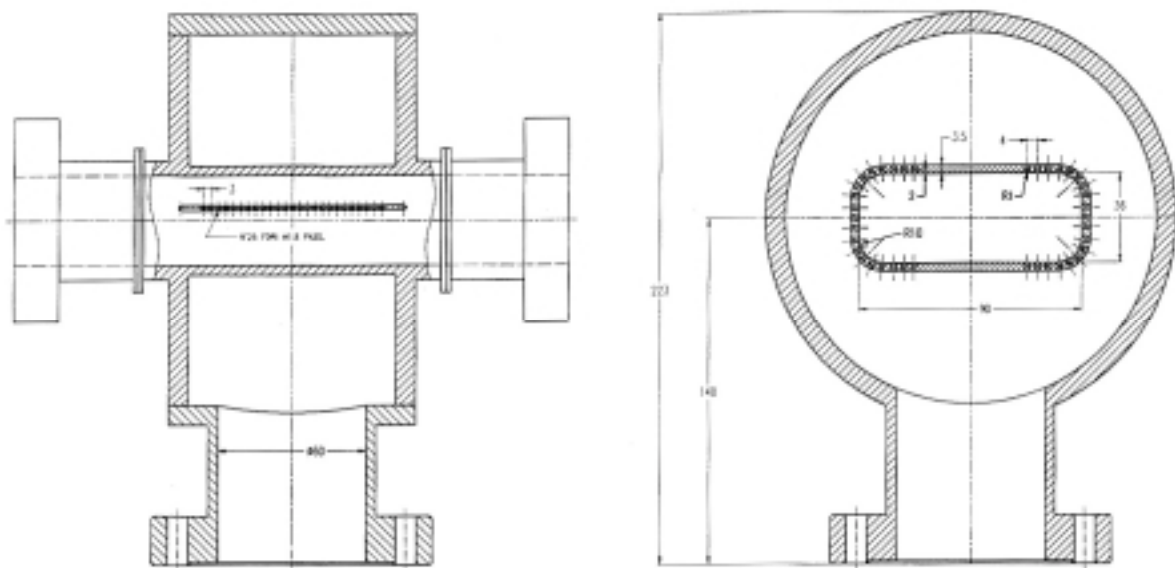

Figure 11: Vacuum port scketch.

In order to decrease further the coupling impedance we exploit properties of the impedance for the rectangular geometry of the beam pipe. The grooves are placed closer to the chamber corners and there are no grooves on the lower and upper desks of the chamber near the symmetry axis.

The impedance of such long narrow slots remains mainly inductive up to rather high frequencies and can be estimated for a rectangular beam pipe as [22]:

$$Z(\omega) = jZ_0 \frac{\omega}{c} \frac{(\alpha_e + \alpha_m)}{b^2} \Sigma^2$$

where the sum of the electric and magnetic polarizabilities for a rectangular slot with the length l and the width w is given by:

$$\alpha_e + \alpha_m = w^3 \left(0.1814 - 0.0344 \frac{w}{l} \right)$$

Here the geometric factor Σ is defined by the series:

$$\Sigma = \sum_{m=0}^{\infty} \frac{\cos\left((2m+1)\pi y_h / b\right)}{\cosh\left((2m+1)\pi x_h / b\right)}$$

with b being the vacuum chamber height; x_h and y_h are the hole coordinates.

Calculations of the impedance for the pumping screen shown in Fig. gives $Z/n = j\ 4.3*10^{-6}$ Ω for a single vacuum ports and respectively about $1.4*10^{-4}\ \Omega$ for all the 32 vacuum ports of the combiner ring. This is a negligible value.

Tapers

In order to minimize the vacuum chamber impedance the vacuum chamber must be as smooth as possible. All the changes in the vacuum chamber cross section have to be provided with gradual transitions – tapers. It is also highly desirable to reduce the number of these vacuum chamber cross section variations.

The vacuum chamber in the CTF3 combiner ring is rectangular, 36x90 mm, with smoothed corners. Since the reutilized quadrupole magnets have large enough apertures it was decided to keep this cross section without changes all along the machine arcs. The only variations of the vacuum chamber cross section take place between the arcs and the wiggler sections and between the arcs and the straight sections needed for injection/extraction.

The wiggler vacuum chamber has the same vertical size as the rest of the arc chamber – 36 mm, but is much wider in the horizontal direction. So, only horizontal tapering is necessary in this case in order to reduce the impedance. Due to the flat rectangular geometry these horizontal tapers are not expected to give any substantial contribution to the machine impedance.

The beam pipe cross section in the straight sections is circular with a diameter equal to the vertical chamber size in the arcs of about 36 mm. Again, only horizontal tapering is needed.

Note at this point, that the whole vacuum chamber has a constant vertical size and a limited number of the horizontal tapers. This allows to reduce the taper impedance contribution to a minimum.

<u>Valves</u>

Since the vacuum chamber is expected to be rather smooth without abrupt cross section variations and there are no narrow chamber sections in the ring, the vacuum conductance of the chamber should be good enough. This gives us a possibility to avoid using valves.

<u>Bellows</u>

There will be 16 bellows providing the vacuum chamber flexibility. We have adopted the so called sliding finger structure for the bellows similar to that used in the KEKB rings [23]. These bellows have small, predominantly inductive, impedance [24] and have proven their reliability working with bunches with the rms size in the millimeter range.

By scaling the impedance of the KEKB bellows to the combiner ring vacuum chamber size we get a very small value of about 10^{-6} Ω per single bellows and $1.6*10^{-5}$ Ω for all the ring bellows, respectively.

<u>Flanges</u>

Another possible source of inductive impedance are flanges. The coupling impedance is due to small narrow gaps created between mounted flange surfaces. Since the gap sizes can be reduced to fractions of mm [25] which are much smaller than the bunch length, we can safely neglect their impedance contribution.

4. Summary

Our preliminary estimates reported in this paper have shown that by careful vacuum chamber design it is possible to keep the energy loss and the energy spread within the design limits. The CSR and the conventional wake fields are evaluated to give almost equal contributions to the energy spread and losses.

The energy spread due to CSR is $\Delta E = \pm$ 0.9 MeV ($\Delta E/E \sim \pm$ 0.5%) for a 2 mm long bunch. It is not reasonable to have bunches shorter than 2 mm in the combiner ring since the energy spread grows fast with the bunch length (faster than $\sim \sigma^{-4/3}$). For a 1 mm long bunch the spread would exceed the acceptable value of $\Delta E/E = \pm$ 1%.

Among vacuum chamber components the 2 RF deflectors and the 36 BPMs give dominant contributions to both energy spread and energy loss. For a 2 mm bunch they are estimated to give about 550 keV of total energy spread considering that the bunch performs 5 turns in the ring. The wake fields created by these components lasts longer than the distance between bunches in the trains and because of that an additional study of the multibunch and multiturn effects is necessary.

The wake fields induced by the extraction kicker are weaker than those of the deflectors and BPMs: the 2 mm bunch with nominal charge of 2.33 nC loses 18 keV and accumulates 34 keV of energy spread after 5 turns.

The contribution of the resistive walls can be small if the vacuum chamber is made of aluminium. The estimated losses in this case are about 12 keV, while the spread does not exceed 36 keV.

Trying to design a smooth combiner ring vacuum chamber it seems to be possible to keep constant the vertical chamber size and reduce the number of lateral (horizontal) tapers. At the present stage of the chamber design these tapers are foreseen only between arcs and two straight sections and between the arcs and two wiggler chamber sections. Such a uniformity of the vacuum chamber cross section provides good vacuum conductance. This allows us to exclude using valves.

The experience acquired during vacuum chamber construction of high current colliders (PEP II, KEKB and DAΦNE) can be successfully applied in order to reduce the coupling impedance of some vacuum chamber components to a minimum. In particular, the inductive impedance of hidden pumping slots, sliding contact bellows, RF screened flanges are expected to be negligible.

5. References

[1] "CLIC RF Power Source: a Novel Scheme of Two Beam Acceleration for Electron-Positron Linear Colliders", Yellow Report CERN 99-06. See also "Proceedings of the First CLIC/CTF3 Collaboration Meeting held at CERN, 3-5 May, 1999", CLIC NOTE 401.

[2] J. B. Murphy, S. Krinsky and R. L. Gluckstern, "Longitudinal Wakefield for an Electron Moving on a Circular Orbit", Particle Accelerators, 1997, Vol. 57, pp. 9-64.

[3] R. L. Warnock and P. Morton, "Fields Excited by a Beam in a Smooth Toroidal Chamber. Part 1: Longitudinal Coupling Impedance.", Particle Accelerators, 1990, Vol. 25, pp. 113-184.

[4] R. L. Warnock, "Shielded Coherent Synchrotron Radiation and Its Effect on Very Short Bunches", SLAC-PUB-5375, Nov. 1990.

[5] R. L. Warnock and K. Bane, "Coherent Synchrotron Radiation and Stability of a Short Bunch in a Compact Storage Ring", SLAC-PUB-95-6837, May 1995.

[6] A. V. Burov and E. A. Perevedentsev, "Coherent Synchrotron Radiation and Its Effect on Bunch Lengthening", in Proceedings of High Energy Accelerator Conference, Hamburg 1992, Vol. 2, pp. 1112-1114.

[7] L. Palumbo, V. Vaccaro and M. Zobov, "Wake-Fields and Impedance", Lecture given at *CAS Advanced Accelerator School*, 20 September - 1 October, Rhodes, Greece, 1993, CERN 95 - 06, 22 November 1995, V.1, pp. 331- 390. See also LNF-94/041 (P), 5 September 1994.

[8] S. Bartalucci et. al., " Measurements and Analysis of Collective Effects in the LEP Electron Positron Accumulator (EPA)", in Proceedings of European Particle Accelerator Conference EPAC88, Rome, June 7 – 11, 1988, Vol.1, pp. 672 – 674.

[9] M. Zobov et. al., "Bunch Lengthening and Microwave Instability in the DAΦNE Positron Ring", DAΦNE Technical Note: BM-3, Frascati, June 7, 1998.

[10] K. Bane and M. Sands, "The Short-Range Resistive Wall Wakefields", SLAC-PUB-95-7074, December 1995.

[11] R. L. Gluckstern, J. van Zeijts and B. Zotter, " Coupling Impedance of Beam Pipes of General Cross Section", CERN SL/AP 92-25 (1992).

[12] D. Alesini et. al., " The RF Deflectors for CTF3", CTFF3 Technical Note-003, Frascati, April 18, 2001.

[13] Y. H. Chin, User's Guide for ABCI Version 8.8, LBL-35258, UC-414, February 1994.

[14] CTFF3 Technical Note, to be published.

[15] S. Battistsi et. al., "Magnetic Beam Position Monitors for LEP Pre-Injector", Proceedings of the 1987 IEEE Particle Accelerator Conference, Washington, March 16-19, 1987, pp. 605 – 607.

[16] CTTF3 Technical Note, to be published.

[17] R. Gluckstern and B. Zotter, "Analysis of Shielding of Charge Particle Beams by Thin Conductors", published in Phys.Rev.ST Accel.Beams 4:024402,2001.

[18] D. Brandt et. al., "Experimental Evaluation of the RF Shielding Properties of a Thin Resistive Layer in a Ceramic Chamber", Proceedings of EPAC 2000, Vienna, Austria, 2000, pp. 1417 – 1419.

[19] S. Battisti, F. Caspers and D. J. Williams, "Mesure de L' Impedance Longitudinale du Prototype no 2 du Capteur de Position Magnetique", PS/LPI/Note/85-04, 1 March 1985.

[20] T. Weiland, "Low Impedance Vacuum Chambers", PEP-II Technical Note No. 59, 1994.

[21] C. K. Ng and T. Weiland, "Impedance of the PEP-II DIP Screen", SLAC-PUB-95-7005, September 1995.

[22] S. S. Kurennoy, "Beam – Chamber Interaction in Accelerators. Methods for Calculating Coupling Impedances ", IFVE-91-158 (Serpukhov, IHEP), Oct 1991. 63pp (in Russian).

[23] Y. Chin and K. Oide, "Impedance and Collective Effects in the KEKB", KEK Proceedings 96-6, August 1995, pp. 1 – 22.

[24] Y. Suetsugu, " Bellows Design and Testing", KEK Proceedings 96-6, August 1995, pp. 189-194.

[25] V. Lollo, private communication.